



Investigation on self-sensing monitoring and resonant control of ultrasonic vibration–assisted cutting

Fuhang Yu¹ · Chen Zhang¹ · Xiaoming Gan¹ · Xin Hu¹

Received: 21 May 2022 / Accepted: 11 January 2023 / Published online: 21 January 2023
© The Author(s), under exclusive licence to Springer-Verlag London Ltd., part of Springer Nature 2023

Abstract

Ultrasonic elliptical vibration-assisted cutting is a precision machining method that improves the surface quality, reduces burrs, and prolongs the life of the tool. However, during the cutting process, the natural frequency of ultrasonic vibration varies with cutting force and contact conditions, which makes the amplitude of the vibration shrink greatly. Consequently, to resist the influence of cutting loads and unpredictable disturbances in the cutting process, an innovative strategy available to stabilize frequency and amplitude with an electro-mechanical conversion model considering hysteresis compensation was proposed. The proposed model is specially designed for the high-frequency ultrasonic vibration device in the actual machining process. First, to compensate for errors caused by the hysteresis nonlinearity in the ultrasonic vibration processing, a method using the Prandtl-Ishlinskii operator to model the hysteresis effect of the ultrasonic device was proposed. The advantage of this method is that it can quickly adapt to the changes in the hysteresis effect of ultrasonic equipment in real time based on the reversible analytical solution of the Prandtl-Ishlinskii operator. Second, a self-sensing circuit was developed to monitor the cutting process of the ultrasonic vibration cutting actuator in real time, which can measure the electrical signal of the piezoelectric ceramic. With a reference to the piezoelectric hysteresis model, a self-sensing model for calculating the amplitude of ultrasonic vibration devices based on electrical signals in real time was established. Finally, a control system to track and control the frequency and amplitude of the ultrasonic vibration process was developed, and the experimental test and the micro-surface cutting experiment of this control system were carried out. It can be seen from the result that the frequency and amplitude of ultrasonic vibration are more robust by using the self-sensing control system, and a significant reduction of 11.47% in the circumferential length error of the machined workpiece was observed.

Keywords Precision manufacturing · Ultrasonic vibration–assisted cutting · Self-sensing · Hysteresis effect · PID control

1 Introduction

The industrial development of aerospace, national defense, and shipbuilding, as well as integrated circuit and semiconductor, applies increasingly higher requirements to the precision and quality of the processing of many key parts. As a typical machining method, ultrasonic vibration cutting is widely used in the precision machining of critical workpieces thanks to its advantages, such as lower cutting force [1] and temperature [2], improved surface quality [3], and prolonged tool life [4]. However, in the actual machining process, the natural frequency of cutting devices varies with

loads, which leads to a substantial drop in the processing amplitude. Besides, there are some external disturbances during the ultrasonic vibration cutting process, which greatly affect the robustness of the machining process. Therefore, it has become a crucial issue in ultrasonic vibration machining to eliminate the influence of cutting loads and unpredictable disturbances and improve the robustness of the cutting system.

In previous studies, mechanical feedback is usually used as a means of measuring vibration fluctuations during ultrasonic vibration processing [5]. HUBBARD et al. [6] proposed a closed-loop monitoring system to improve the machining quality of the machining process. Chua et al. [7] developed a framework for the development of a monitoring and inspection system in the additive manufacturing process by establishing the correlation between the process parameters and process signatures. Woronko et al. [8] compensated

✉ Chen Zhang
meczhang@nuaa.edu.cn

¹ Nanjing University of Aeronautics and Astronautics,
Nanjing 210016, China

the nonlinear error in the working process of the actuator by using the sliding film control algorithm. In summary, in these methods, additional high-precision sensors are often required, which inevitably leads to system redundancy and higher processing costs. In addition, during the machining process, the position of the sensor usually interferes with the machining by occupying the installation space of the cutting tool and the machining workpiece, which causes great inconvenience to the machining.

To solve these problems, more and more research is carried out for sensorless monitoring and control of the vibration of piezoelectric transducers. Shamoto et al. [9] used piezoelectric ceramics installed on the actuator of the vibration device as a feedback sensor to eliminate the crosstalks between the two directional vibrations of the stepped vibrator excited in the same bending mode in two directions. The experiment shows that an ultraprecise mirror surface with a shape accuracy of less than 0.2 pm is obtained by using the system. Yin et al. [10] designed a novel single-driven ultrasonic elliptical vibration cutting device with a complex beam horn. The experimental results show that, compared to conventional cutting (CC), the cutting force and surface roughness of the cutting process are reduced by this device. Bazghaleh et al. [11] proposed a new type of charge amplifier, which combines the grounded-load digital charge amplifier (GDCDE) and the artificial neural network (ANN) to estimate displacement over a wide bandwidth and overcome drift. According to the experimental results, the hysteresis effect of this charge amplifier is reduced by 91% compared with the traditional voltage amplifier. However, this charge amplifier has the problem of drift during long-term operation. In addition, some research showed that the relationship between charge and displacement of piezoelectric ceramics is more linear than the relationship between voltage and displacement [12]. By this theory, Minase et al. [13] developed a hardware-free charge control feedback controller by using the charge-driven method and estimated the displacement of the piezoelectric drive device based on the charge information. In this control method, the linear relationship between charge and displacement is used to simplify the control system. Then, a compensation model for static parameters was established by Ryba et al. [14] based on polynomial equations, and the inverse model was directly simulated in this model. Finally, the experimental results for tracking both triangular and sinusoidal signals were presented to verify the static parameter model. Instead of measuring the velocity with a sensor, Tanaka et al. [15] utilized the electro-mechanical coupling effect of the piezoelectric device and fabricated a sensorless self-excitation system for a macrocantilever based on DSP. The validity was assessed through experiments. Chen et al. [16] proposed a high-precision driving method for a piezoelectric driving platform by using the electro-mechanical model of the piezoelectric

transducer. The position or displacement sensors were not required in this method, and a built-up charge sensing circuit can be used to detect the amount of charge of the piezoelectric transducer.

To solve the problem that the vibration state of ultrasonic vibration devices changed with load in the actual cutting process, the relationship between the input electrical signal and the output displacement was studied. Liaw et al. [17] proposed an enhanced sliding mode motion tracking control methodology for piezoelectric actuators to track desired motion trajectories. This methodology was established to accommodate parametric uncertainties, nonlinearities including the hysteresis effect, and other disturbances. Zhu et al. [18] constructed an estimated model of the elliptical cutting device considering cutting load by using a displacement sensor. In this method, the cutting force was estimated by comparing the measured displacement with the estimated free displacement. Zhang et al. [19] developed a tool-workpiece thermocouple system for the temperature measurement of high-speed ultrasonic vibration cutting Ti-6Al-4 V alloys. Moreover, the robustness of ultrasonic vibration cutting devices in the process of machining has been widely concerned by researchers. Gao et al. [20] proposed a sensorless method to track and control the frequency and amplitude of the machining process. They designed a Kalman filter observer to estimate the velocity of vibration and the phase between the supply voltage and current, so as to achieve the stability of vibration in the cutting process. However, the hysteresis nonlinearity of the piezoelectric transducer was not considered in this linear model. A self-sensing method was proposed by Mansour et al. [21] for piezoelectric transducers, which can be used to estimate displacement and force by measuring voltage and charge. Zhang et al. [22] researched the influence of mechanical compliance of mounting clamps on the performance of the high-frequency piezoelectric ultrasonic transducer. The experiments showed that the electromechanical coupling coefficient and the quality factor of the transducer increase with the increment in the mechanical compliance of the clamp. Aiming at the difficult motion decoupling of ultrasonic vibration devices, Yang et al. [23] presented a new optimization design method of ultrasonic elliptical vibration cutting tool with dual longitudinal generators to create a well-decoupled elliptical trajectory. The precise control of vibration is significant to improve the machining quality in the process of ultrasonic vibration cutting. The Preisach model was utilized by Ge [24] to model the hysteresis and nonlinearity of the piezoelectric transducer, of which the numerical inverse model was used as the basis to establish the feedforward controller before proposing a composite control method to improve the tracking precision of the system. Viswamurthy et al. [25] used the Preisach model to characterize the hysteresis in a piezostack actuator for

helicopter vibration control. However, the Preisach model is not analytically reversible; therefore, the approximate inverse model of the Preisach model can only be obtained through numerical methods, such as the look-up table method or iterative algorithm. After that, by considering the dynamic creep effect, the tracking error of the piezoelectric ceramic transducer was reduced by an order of magnitude. Due to the characteristics of the PI model, that is, the only existing analytical inverse model, it is also used by researchers in feedforward compensation research [26]. Rakotondrabe et al. [27] designed a hysteresis compensation controller based on the inverse multiplicative scheme. There are some advantages like simplicity and intuitiveness in this hysteresis model, but also some disadvantages, such as long calculated time, a complicated system structure, and the accuracy of the model depending on the initial state. Lin et al. [28] realized hysteresis compensation of biaxial piezoelectric driven stage by using generalized Duhem model in feedforward control mode. In addition, Xu [29] developed a model based on least squares support vector machines for the identification and compensation of the hysteresis effect. Although the complex calculation of the inverse model is avoided in this hysteresis model, the analytical inverse model cannot be obtained due to the complexity of the hysteresis model.

In conclusion, there are three vital problems that remain unresolved in the current control method for the ultrasonic vibration–assisted cutting process. First, the output displacement of the ultrasonic vibration cutting device is also measured by using a dedicated sensor, which greatly increases the processing cost and squeezes the available space in the processing. Second, due to the high-frequency fluctuation of displacement in ultrasonic vibration machining, the compensation of its hysteresis effect was always a difficult problem in the case of estimating the displacement of the ultrasonic vibration process. Third, because the ultrasonic vibration device is affected by the load during the working process, its actual natural frequency is different from the operating frequency. It affects the trajectory of vibration and reduces the machining quality.

Facing the problems above, there are three solutions proposed in this paper. First, a self-sensing circuit is established to monitor the real-time electrical signal of the device during the processing, which replaces the function of dedicated sensors. Second, considering the high-frequency characteristics of the ultrasonic device, a hysteresis model is established based on the PI (Prandtl-Ishlinskii) operator. Based on the reversible analytical solution of this model, a feedback compensation algorithm was proposed to track the rapid change of ultrasonic devices considering the hysteresis effect. Finally, with regards to the influence of processing load on cutting devices, a closed-loop control system is constructed to keep the device in the resonant state, which is not affected by the load during machining.

In this paper, a self-sensing monitoring and closed-loop control system of the ultrasonic vibration cutting process was proposed. What is more, a compensation method of the control system for the hysteresis effect based on the PI model is proposed. This paper is organized as follows: In Section 2, a method for fitting and compensating the hysteresis voltage based on the PI model is present. In Section 3, an electro-mechanical conversion model of the vibrating cutting device is discussed in combination with the piezoelectric hysteresis effect. Subsequently, the feasibility and accuracy of this model were verified through experiments. In Section 4, a self-sensing strategy and closed-loop control system considering the piezoelectric hysteresis effect of the ultrasonic device are proposed. In Section 5, a cutting experiment is carried out to verify the accuracy of this self-sensing monitoring and closed-loop control system proposed in this paper. In Section 6, the analysis of the experimental results for the self-sensing control system is summarized.

2 Hysteresis compensation of ultrasonic elliptical vibration cutting device

Due to the hysteresis effect of the piezoelectric transducer, the input signals and output trajectory present a nonlinear relationship, which has an adverse effect on the precise control of vibration. Moreover, there are higher requirements for real-time modeling of hysteresis effects affected by high frequencies in ultrasonic vibration machining. However, the hysteresis effect of the ultrasonic vibration device is usually ignored in the existing research. In this section, a method for modeling and compensating the hysteresis voltage is established based on the PI model. Then, by testing the ultrasonic elliptical vibration cutting device, the curve of hysteresis voltage is obtained. Finally, an experiment was performed to verify the accuracy of the model.

2.1 Electro-mechanical conversion model of piezoelectric transducer

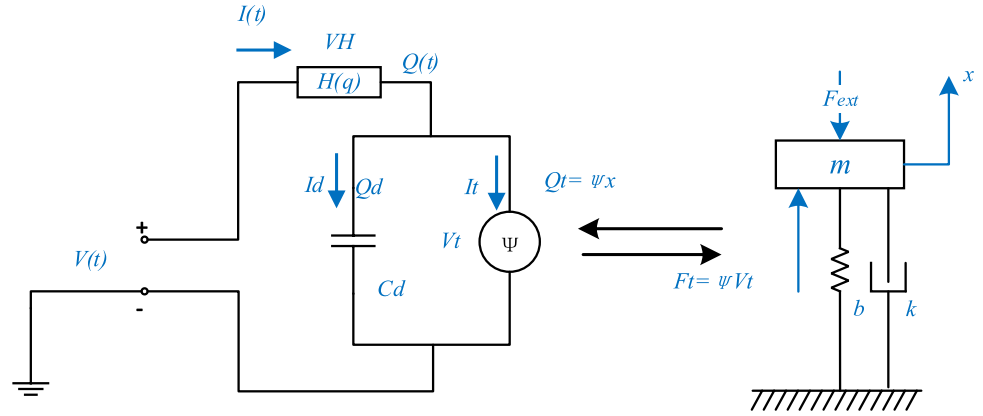
The electro-mechanical equivalent method is effective for designing and analyzing piezoelectric transducers. In order to obtain the relationship between input and output of piezoelectric transducer, the electrical and mechanical properties of piezoelectric ceramics were analyzed. The equivalent circuit of a piezoelectric transducer can be described as shown in Fig. 1.

A simplified electromechanical model is shown in Fig. 1. The linear constitutive relationship of a piezoelectric transducer can be expressed as:

$$F_t = \psi V_t \quad (1)$$

$$Q_t = \psi x \quad (2)$$

Fig. 1 Nonlinear electromechanical conversion model of piezoelectric transducer



where the constant ψ represents the electro-mechanical conversion coefficient, which represents the mapping relationship between the supply voltage $V(t)$ and the driving force F_r , or the mapping relationship of the vibration velocity \dot{x} and transforming current I_r . Its unit can be N/V or C/m. x represents the output displacement, $V(t)$ represents the supply voltage at time t , and $Q(t)$ represents the charge from the beginning to the time t .

From this, the relationship of the displacement and the electrical signal can be expressed as:

$$x = \frac{1}{\psi} [Q(t) - C_d(V(t) - V_H)] \tag{3}$$

where V_H stands for hysteresis voltage, which is the voltage loss due to hysteresis nonlinearity. Its value can be calculated by measuring the charge $Q(t)$ through the piezoelectric ceramic. C_d represents the static equivalent capacitance of the piezoelectric ceramic. The specific calculation will be discussed in the next section.

2.2 Hysteresis effect of ultrasonic elliptical vibration cutting device

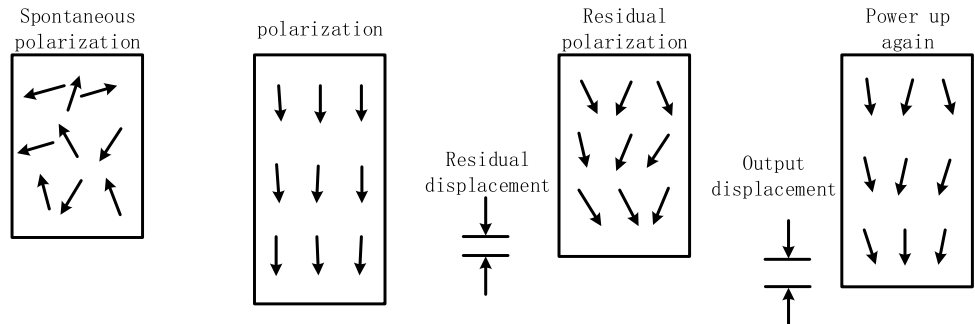
The core structure of transducers is piezoelectric ceramics. Research shows that piezoelectric material (such as lead zirconate titanate (PZT)) is a kind of polar material, and

its electric dipole moment is caused by the arrangement of many electric dipoles inside the crystal. The polarization process can be divided into four stages, i.e., spontaneous polarization, polarization, residual polarization, and power up again. In the case that the piezoelectric ceramic is not affected by the external electric field, the vector sum of its electric dipole moment is zero, and the piezoelectric ceramic is spontaneously polarized at the same time. When piezoelectric ceramics are exposed to an electric field, the orientation of the electric dipoles will approach that of the applied electric field gradually. The result of this phenomenon is that a single crystal and all adjacent crystals expand in the direction of the applied electric field. This process is called polarization. When the electric field is removed, the electric dipole is in a state between nonpolarization and polarization, which is called remnant polarization. Then, it waits for power-up again. This polarization process is shown in Fig. 2.

It can be seen from Fig. 2 that the polarization process can be completed and displacement can be output when an external electric field is applied to the piezoelectric ceramic for a period of time. Due to this phenomenon, there is a time lag between the applied input voltage and the output displacement, which is the hysteresis effect, as shown in Fig. 3.

Affected by many factors (such as structure, material, and temperature), the hysteresis curves of piezoelectric transducers are different. In order to investigate the relationship between the electrical signal and the output displacement

Fig. 2 Polarization principle of piezoelectric materials



of the ultrasonic vibration device, a series of experiments are carried out in this paper. The experimental setup of the ultrasonic vibration device is shown in Fig. 4, and the experimental facilities are shown in Table 1.

According to the acquisition experiment, the supply voltage and output displacement of the ultrasonic elliptical vibration cutting device were measured. The voltage-displacement characteristic curve of the ultrasonic elliptical vibration cutting device is shown in Fig. 5, and the voltage-charge characteristic curve is shown in Fig. 6.

It can be seen from Fig. 5 that, when the AC voltage changes, the output displacement is related to the rise and fall of the voltage. If we connect the displacement point at extreme voltages with a dashed line in Fig. 5a, it represents the approximate average displacement over a period. When the amplitude of voltage rises, the displacement is lower than the average displacement. When the voltage drops, the displacement is higher than the approximate average displacement. This shows hysteresis between voltage and displacement. The charge curve also shows the same regularity in Fig. 6. So from Eq. (3), the formula of hysteresis voltage V_H is as follows:

$$V_H = \frac{\psi x + C_d V(t) - Q(t)}{C_d} \tag{4}$$

For the ultrasonic vibration–assisted cutting device, the mechanical and electrical conversion coefficient changes with the different structure arrangement compared with the single piezoelectric transducer unit. The detailed process of the identification of conversion coefficient k is shown in Section 3. The hysteresis voltage of the two-dimensional elliptical vibration cutting device can be expressed as:

$$V_H = \frac{kx + C_d V(t) - Q(t)}{C_d} \tag{5}$$

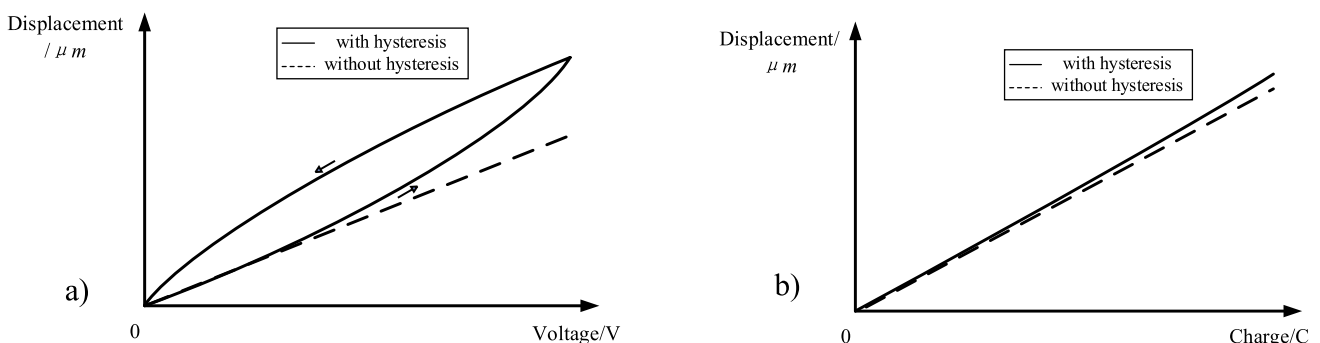


Fig. 3 Hysteresis characteristic curve of piezoelectric transducer: **a** voltage-displacement characteristic curve and **b** charge-displacement characteristic curve



Fig. 4 Acquisition and analysis of electrical signal and displacement signal of ultrasonic vibration device

The static capacitance C_d of the device can be obtained by impedance analysis. In this paper, Agilent 4294A impedance analyzer was used to test the ultrasonic vibration device, as shown in Fig. 7. After testing, the static capacitance $C_d=794$ pF of the ultrasonic vibration device used in this paper is obtained.

By substituting the measured voltage-charge data of Fig. 6 into Eq. (5) for calculation, the hysteresis voltage and charge characteristic curve of this device can be obtained as shown in Fig. 8.

It can be seen from Fig. 8 that there is also a hysteresis relationship between the hysteresis voltage and the charge. The hysteresis relationship in Fig. 8 is similar to that of the voltage-displacement hysteresis curve. Therefore, it is possible that there is a linear relationship between charge and displacement. So, in order to obtain the relationship between charge and output displacement in the device, the hysteresis model between voltage and charge is established first.

2.3 Hysteresis modeling based on PI model

Although the voltage of a device can be acquired during the actual machining process, the relationship between voltage and charge is difficult to obtain due to hysteresis effects. Since the PI (Prandtl-Ishlinskii) operator is a numerical model with explicit reversible solutions, this operator is used

to model the hysteresis effect of the piezoelectric transducer. The PI model is a phenomenological hysteresis model based on hysteresis operators, which can be seen as a superposition of several operators with different thresholds. Each operator has the basic characteristics of hysteresis. Theoretically, a hysteresis curve of arbitrary shape can be fitted by weighting the operator appropriately, as shown in Fig. 9.

The formula of the PI model can be expressed as:

$$Q(t) = \sum_{i=1}^n \omega_i \cdot P_i(t) = \sum_{i=1}^n \omega_i \cdot \max\{U(t) - r_i, \min\{U(t) + r_i, P_i(t - T)\}\} \quad (i = 1, 2, \dots, n) \quad (6)$$

where $Q(t)$ is the output charge of the PI model at time t , $U(t)$ is the input voltage of the PI model at time t , ω_i is the weight of the PI model, and r_i is the threshold of the PI model. And $r_i = [r_0, \dots, r_n]^T$, n are the number of Play operators, and T is the time interval.

For the PI operator, the weight ω and threshold r can affect the shape and size of the hysteresis model. The accuracy of this model can be measured by using the sum variance, so the parameters of this hysteresis model can be identified as shown in Table 2.

To test the accuracy of this model, the data of Table 1 was substituted into the model; the measured data and simulated data of charge-hysteresis voltage are shown in Fig. 10.

In order to evaluate the accuracy of this hysteresis model quantitatively, the root mean square error (e_{rmse}), maximum error (e_m), and maximum relative error (δ_m) were calculated. The results are shown in Table 3.

It can be seen from Table 3 that within the range of the excitation voltage amplitude from 300 to 500 V, the error of the hysteresis model is relatively small and stable. With the increase of the excitation voltage amplitude, the deviation increases. At the excitation voltage amplitude of 600 V, the deviation between the measured data and the model simulation experiences a large change, and the error curve appears to drift significantly. From the perspective of the maximum relative error, when the excitation voltage is below 500 V, the maximum relative error remains below 10%. Only when the maximum relative error is 600 V, there is a significant

increase. Therefore, it can be explained that the hysteresis model has a better modeling effect at a relatively low voltage.

Based on the inversion of the PI model, hysteresis voltage can be expressed as:

$$U(Q(t)) = \sum_{i=1}^n \omega'_i \cdot \max\{q(t) - r'_i, \min\{q(t) + r'_i, U(t - T)\}\} \quad (7)$$

where $U(Q(t))$ is the hysteresis voltage after hysteresis compensation, ω'_i is the weight of the hysteresis inverse model, and r'_i is the threshold of the hysteresis inverse model.

3 Electro-mechanical conversion model and self-sensing strategy for the ultrasonic vibration-assisted cutting device

In ultrasonic elliptical vibration-assisted processing, the real-time physical state of an ultrasonic vibration device (such as tool displacement, device amplitude, and vibration frequency) has a direct impact on the processing quality of the workpiece. Therefore, in precision engineering, it is necessary to monitor the physical state of the machining process. Although common monitoring methods are simple, including force sensors, displacement sensors, and laser vibrometers, they are expensive and require a special installation location, which will increase the complexity of the system to a certain extent. In this section, the electro-mechanical conversion model of the vibrating cutting device is established, considering the piezoelectric hysteresis effect described in the previous section. Furthermore, a self-sensing system for acquiring real-time current and voltage of devices is designed to verify the accuracy of this model.

3.1 Electro-mechanical conversion model of ultrasonic elliptical vibration cutting device

In this paper, the two-dimensional ultrasonic elliptical vibration-assisted cutting device is our research object. The

Table 1 Equipment information of signal acquisition experiment

	Version	Feature
Computer	PC	Provides operation screens for setting parameters and displaying results
Controller	NI-USB6361X	Operation control system
Signal acquisition device	Design by ourselves	Collect voltage and current signals
Voltage amplifier	TERK PZD700A	The excitation voltage signal is amplified
Capacitance displacement sensor	Microsense 5504	Measure the output displacement of ultrasonic vibration device
Signal conditioning module	Microsense 5300	Signal processing

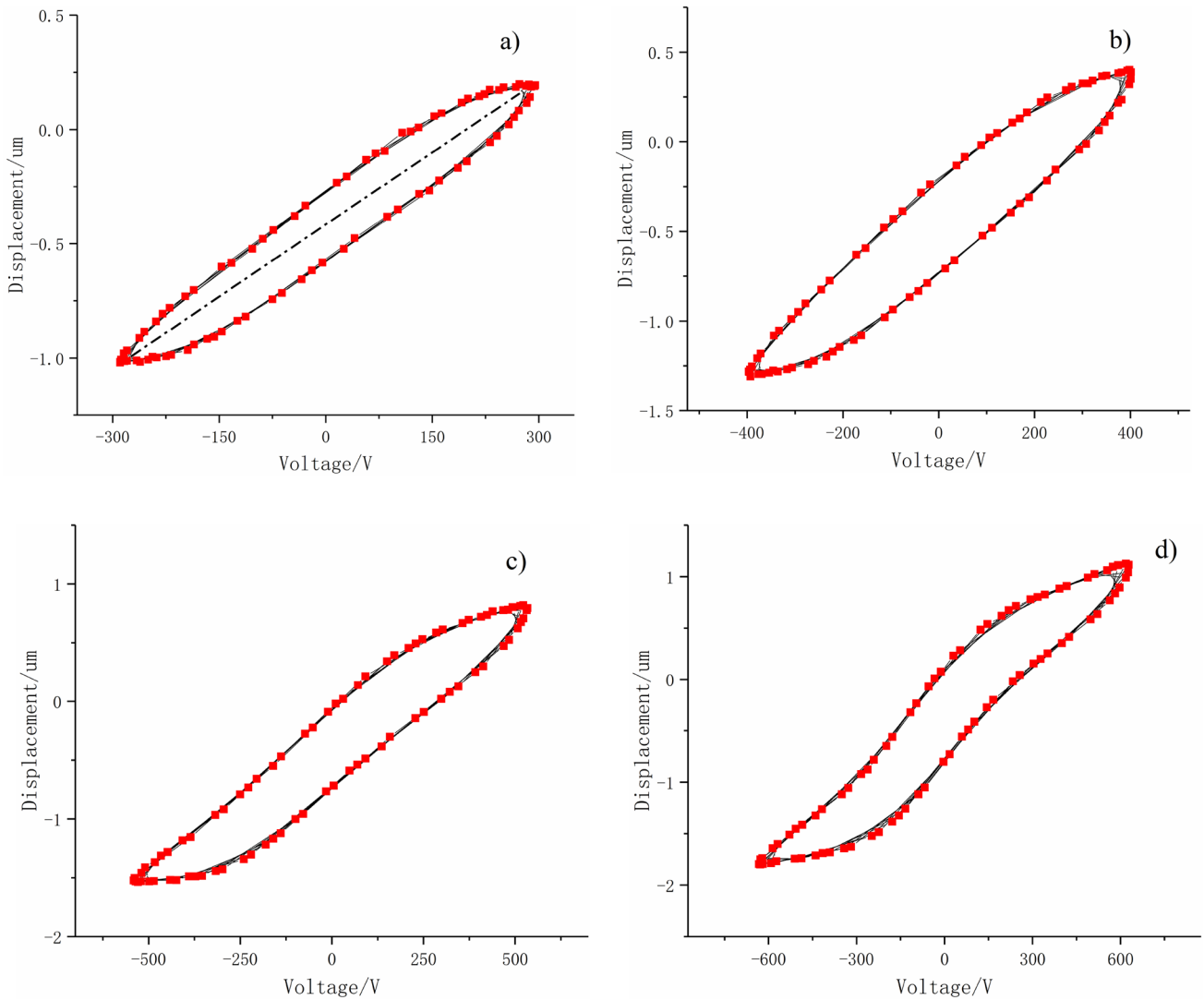


Fig. 5 The voltage-displacement characteristic curve of ultrasonic device: **a** voltage amplitude 300 V, **b** voltage amplitude 400 V, **c** voltage amplitude 500 V, and **d** voltage amplitude 600 V

structure of this device is shown in Fig. 11. Other devices can be specifically analyzed based on their own structure.

The schematic diagram of the two-dimensional ultrasonic elliptical vibration cutting device is shown in Fig. 11, which includes two sets of piezoelectric transducers. By applying excitation voltage, the two sets of piezoelectric ceramics can vibrate in two directions, so an elliptical trajectory is formed at the tooltip finally. The kinematic model of a two-dimensional ultrasonic elliptical vibration cutting device is shown in Fig. 12.

In Fig. 12, assuming the displacement of piezoelectric transducers 1 and 2 are x_A and x_B , respectively, the vibration frequency of two sets of piezoelectric transducers is f . Then, the kinematic model of tool vibration can be expressed as:

$$\begin{cases} x_t = \frac{\sin \frac{\theta}{2}}{2\psi} [Q_A(t) - Q_B(t) - C_d(V_A(t) - V_{HA}) \\ + C_d(V_B(t) - V_{HB})] - \sqrt{a^2 + b^2} \sin(\theta_t - \theta_{t0}) \\ y_t = \frac{\cos \frac{\theta}{2}}{2\psi} [Q_A(t) + Q_B(t) - C_d(V_A(t) - V_{HA}) \\ - C_d(V_B(t) - V_{HB})] - \sqrt{a^2 + b^2} \cos(\theta_t - \theta_{t0}) \end{cases} \quad (8)$$

$$\theta_t = \frac{\pi}{2} + \arctan \left\{ \frac{\cos \frac{\theta}{2} [Q_B(t) - Q_A(t) + C_d(V_A(t) - V_{HA}) - C_d(V_B(t) - V_{HB})]}{2c - \sin \frac{\theta}{2} [Q_A(t) + Q_B(t) - C_d(V_A(t) - V_{HA}) - C_d(V_B(t) - V_{HB})]} \right\} \quad (9)$$

In this research, transducer 1 and transducer 2 are driven with the same supply voltage, so $Q_A(t) = Q_B(t)$, $V_{HA} = V_{HB}$, $V_A(t) = V_B(t)$. The coordinates $P_t(x, y)$ of tool point P_t can be simplified as:

Fig. 6 The voltage-charge characteristic curve of the ultrasonic device: **a** voltage amplitude 300 V, **b** voltage amplitude 400 V, **c** voltage amplitude 500 V, and **d** voltage amplitude 600 V

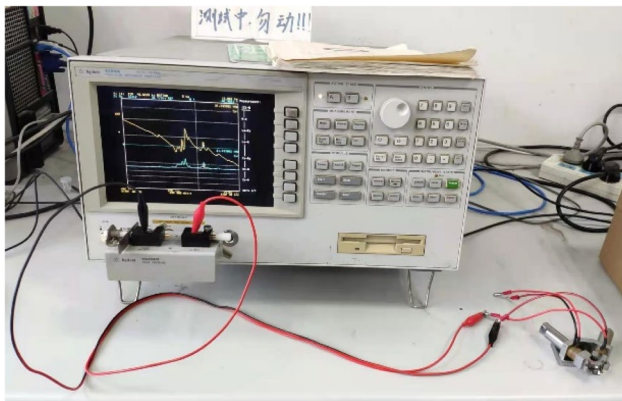
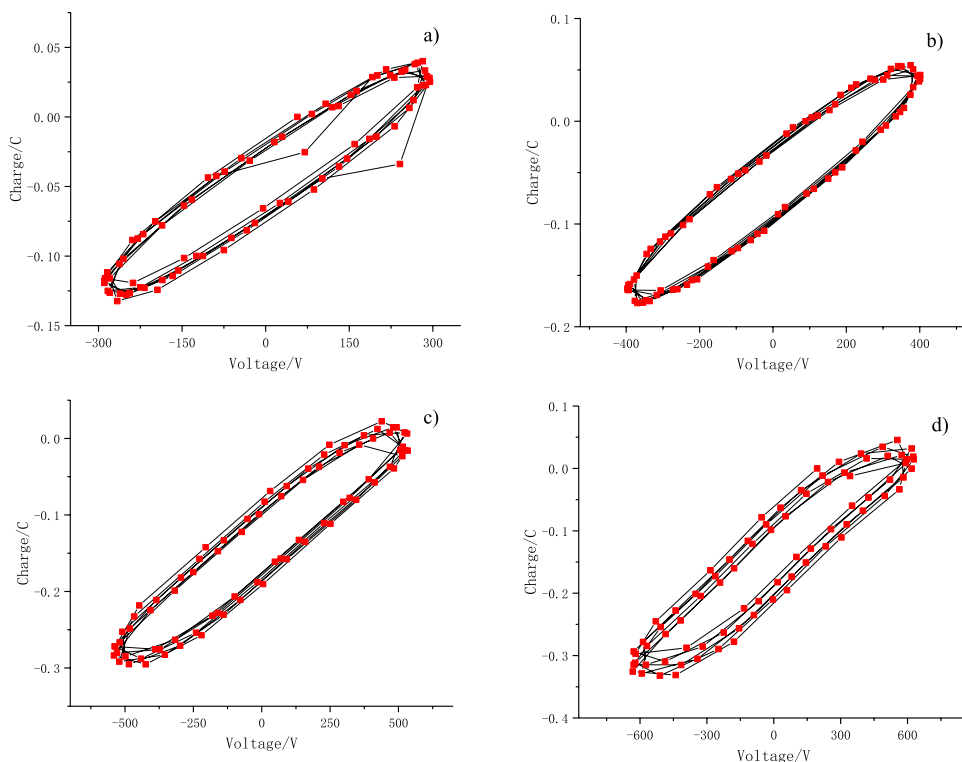


Fig. 7 Impedance measurement of ultrasonic elliptical vibration turning device

$$\begin{cases} x_t = b \\ y_t = \frac{1}{\psi} [Q(t) - C_d(V(t) - V_H)] \cos \frac{\theta}{2} + a \end{cases} \quad (10)$$

Therefore, in this paper, the displacement x of tooltip for a vibration-assisted cutting device can be expressed as:

$$y = y_2 - y_1 = \frac{1}{\psi} [Q(\Delta t) - C_d(V(\Delta t) - V_H)] \cos \frac{\theta}{2} = k [Q(\Delta t) - C_d(V(\Delta t) - V_H)] \quad (11)$$

Based on the established electromechanical conversion model, it is a crucial issue to obtain the total charge $Q(t)$ and total voltage $V(t)$ of a piezoelectric transducer. However,

these signals required cannot be obtained directly during the processing. Therefore, an acquisition system should be designed to collect the voltage and current signals of piezoelectric ceramic in the vibrating process. The acquisition circuit shown in Fig. 13 was designed to measure the current and voltage in real time.

During the vibration process, the electrical information of piezoelectric ceramics changes with loads in real time. Since the internal electrical parameters of piezoelectric ceramics are not convenient for direct measurement, the electrical signals of piezoelectric ceramics are collected according to the acquisition circuit designed in Fig. 13. Then, the electrical information of piezoelectric ceramics can be calculated according to the voltage relation.

3.2 Parameter identification of acquisition system and analysis of results

The two-dimensional ultrasonic elliptical vibration cutting device was taken as the object of this research. After pre-calibration, the resonance frequency of this cutting device used was 18.4 kHz. The equipment information is shown in Table 4, and the acquisition and processing of self-sensing signals are shown in Fig. 14.

During the vibrating process, according to the self-sensing processing shown in Fig. 14, the voltage and current of piezoelectric transducers were collected by the acquisition system. While collecting the voltage

Fig. 8 Hysteresis voltage-charge characteristic curve of ultrasonic device: **a** voltage amplitude 300 V, **b** voltage amplitude 400 V, **c** voltage amplitude 500 V, and **d** voltage amplitude 600 V

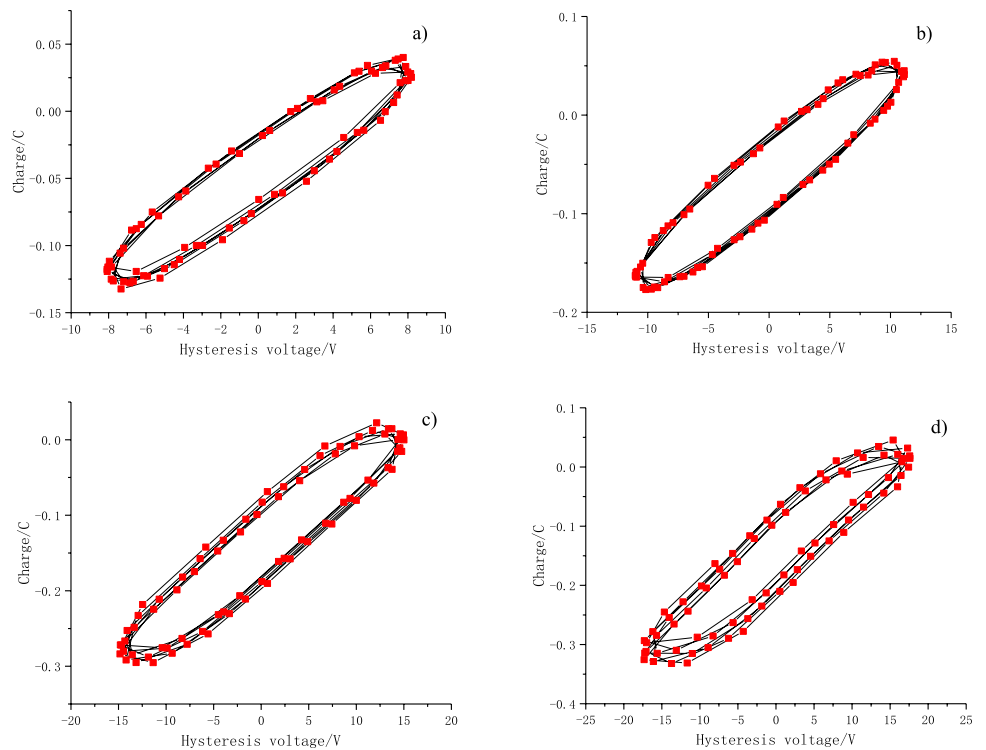
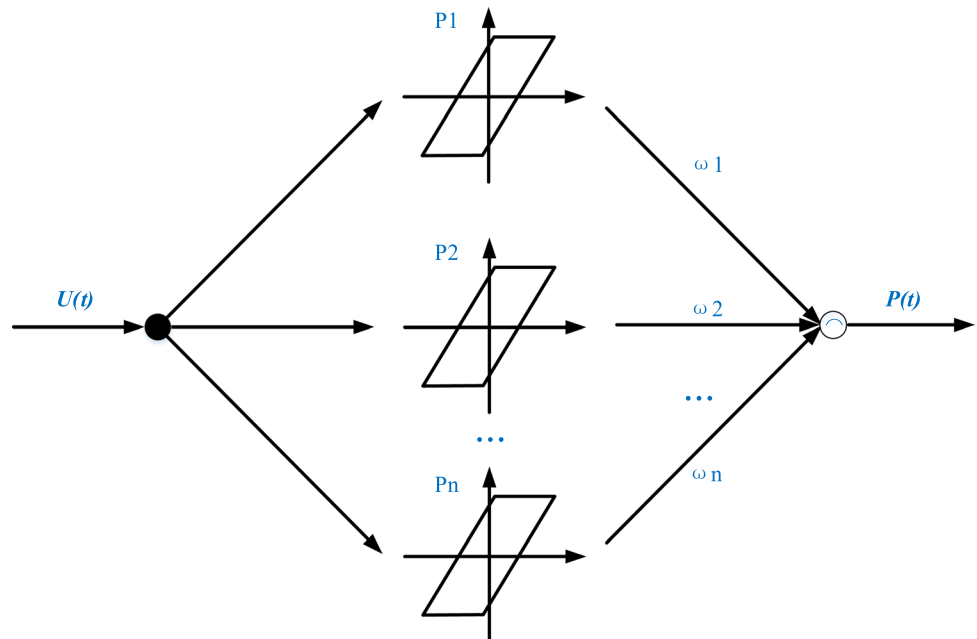


Fig. 9 Schematic diagram of PI



and current signals, the Microsense 5504 capacitive displacement sensor was used to measure the actual displacement of a tooltip. By calculating the self-sensing current, the charge Q_t of piezoelectric transducers in time t can be obtained. Therefore, based on

the self-sensing acquisition system and the hysteresis model established in the previous section, the real-time signals of piezoelectric ceramics are monitored and calculated. The charge-displacement characteristic curve is shown in Fig. 15.

Table 2 Parameters of PI model

Excitation voltage	300 V		400 V		500 V	
	r_i	ω_i	r_i	ω_i	r_i	ω_i
1	0	0	0	0	0	0
2	1	0.00602	1.375	0.00523	1.875	0.00671
3	2	0.00236	2.75	0.00331	3.75	0
4	3	0	4.125	0	5.625	0.00358
5	4	0.00088	5.5	0.00171	7.5	0
6	5	0	6.875	0	9.375	0
7	6	0.00747	8.25	0.00638	11.25	0.00613
8	7	0	9.625	0	13.125	0

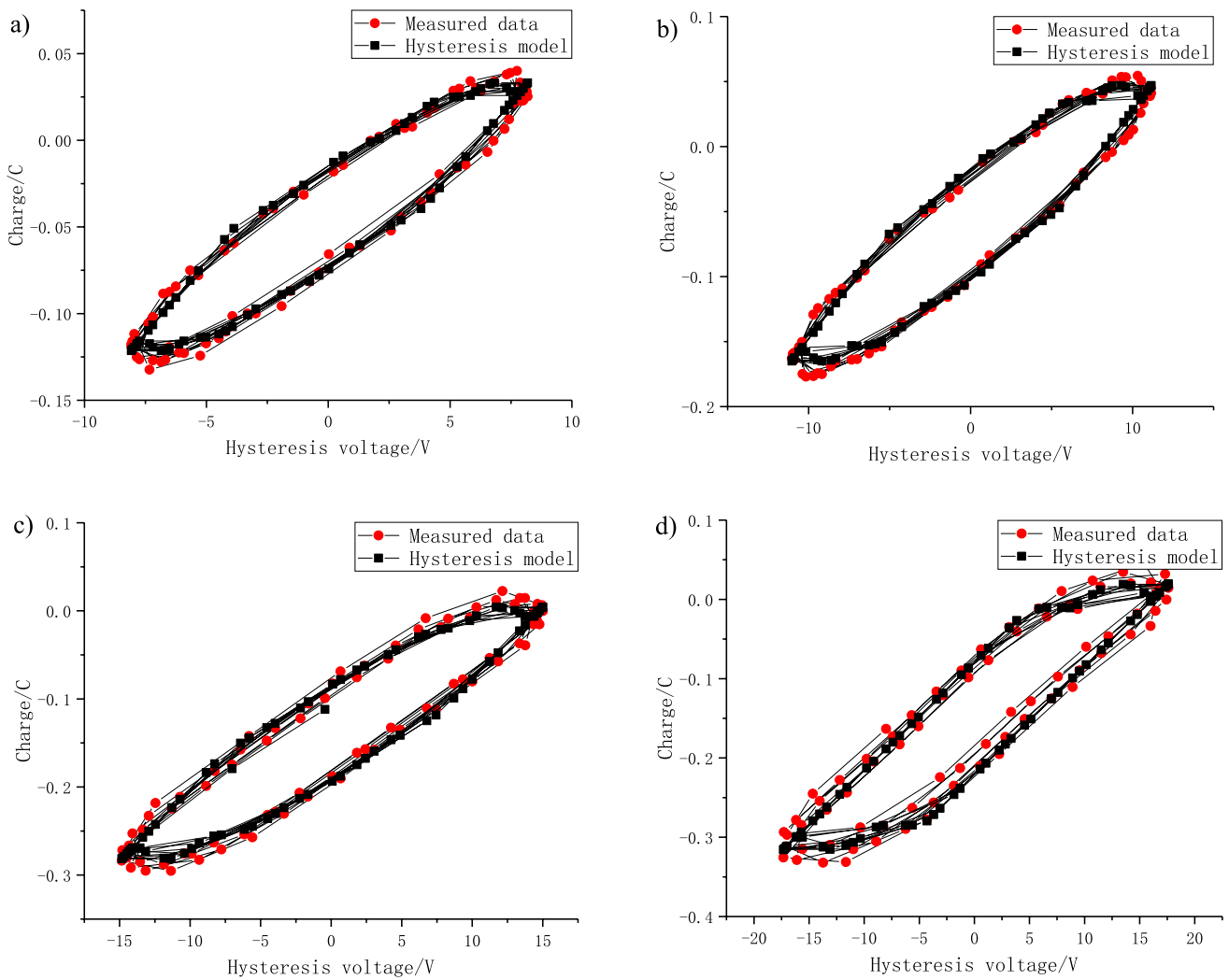
**Fig. 10** The measured data and simulated data of charge-hysteresis voltage: **a** voltage amplitude 300 V, **b** voltage amplitude 400 V, **c** voltage amplitude 500 V, and **d** voltage amplitude 600 V

Table 3 Error comparison of hysteresis models with different excitation voltage amplitude

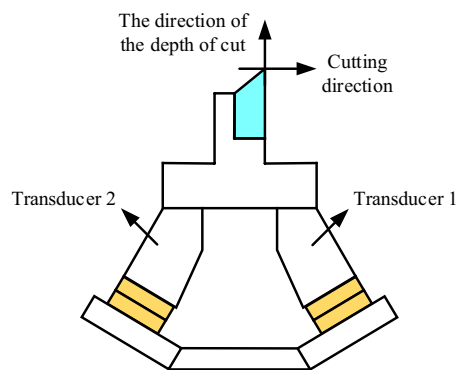
Voltage amplitude	300 V	400 V	500 V	600 V
Root mean square error (e_{rmse}/C)	0.006	0.007	0.011	0.016
Maximum error (e_m/C)	0.015	0.020	0.024	0.039
Maximum relative error ($\delta_m/\%$)	8.33	7.66	9.57	16.21

It is not difficult to see from Fig. 15 that there is a linear relationship between the charge and the output displacement of piezoelectric ceramics. So finally, the nonlinear relation between electrical signal and displacement of a piezoelectric transducer is transformed into a linear relationship based on the electromechanical transformation model and hysteresis model established above. Furthermore, the conversion coefficient k of piezo-electric transducers represents a conversion relationship of charge and displacement. For different excitation voltages, the response time of electric dipole in piezoelectric materials is also different due to the electric field intensity. Therefore, the conversion coefficients of different supply voltages are slightly different. According to the linear relationship shown in Fig. 14, the identification results of conversion coefficients for different voltage amplitudes are shown in Table 5.

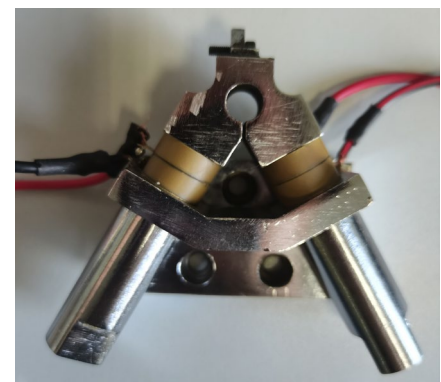
Substituting the coefficient k into Eq. (11) and combining it with the hysteresis model in Section 2, the system parameters in this electromechanical conversion model are calibrated. By monitoring the electrical signal of a piezoelectric transducer in real time, the estimated value of displacement was calculated. The comparison of measured and estimated displacement is shown in Fig. 16.

In order to evaluate the accuracy of this model quantitatively, the errors of actual displacement and estimated displacement were selected as evaluation indexes. The calculation results are shown in Table 6.

Fig. 11 Two-dimensional ultrasonic elliptical vibration cutting device



a) Schematic diagram of the device



b) The actual device

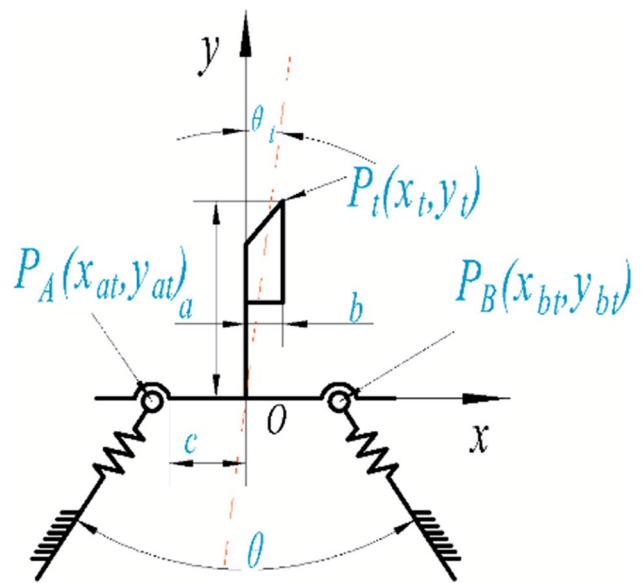


Fig. 12 Kinematic model of two-dimensional ultrasonic elliptical vibration cutting device

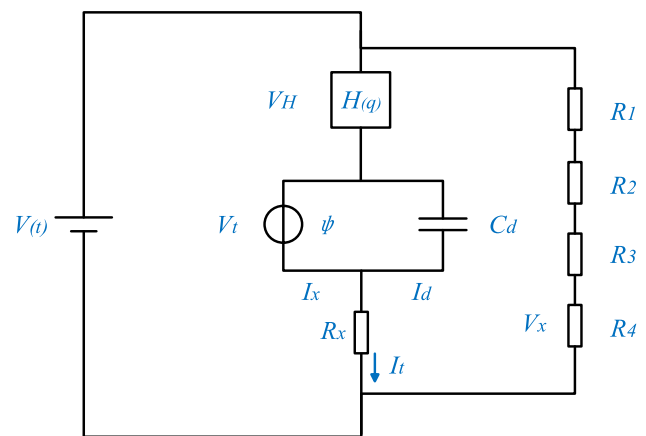


Fig. 13 The acquisition circuit of ultrasonic vibration devices

It can be seen from Table 6 that although the actual and estimated displacement increase with the excitation voltage amplitude, their displacement amplitudes are very close. The maximum error of this estimated displacement is only 1.47%. Therefore, it can be determined that the electro-mechanical model established in this paper is accurate.

4 Frequency and amplitude control system effect of ultrasonic vibration cutting devices

Considering the hysteresis effect, the electro-mechanical conversion model established above is used to model the relationship between the state parameters (displacement) and internal signals (voltage and current signals) of ultrasonic elliptical vibration cutting devices. In this section, based on the model established above, a frequency and amplitude control system for ultrasonic elliptical vibration cutting is designed to stabilize the amplitude and frequency of devices. Furthermore, a self-sensing method to estimate the displacement, frequency, and other information of ultrasonic elliptical vibration cutting devices is designed, which solves the problem of monitoring the state of ultrasonic vibration devices.

It was discovered that there is a mapping relationship between electric signal and working state during the working process of piezoelectric transducers. Many models were proposed to describe the relationship of piezoelectric. At

present, the linear constitutive relation of piezoelectric ceramics proposed by the Institute of Electrical and Electronics Engineers (IEEE) in 1987 is widely recognized:

$$S = s^E T + dE \tag{12}$$

$$D = dT + \epsilon^T E \tag{13}$$

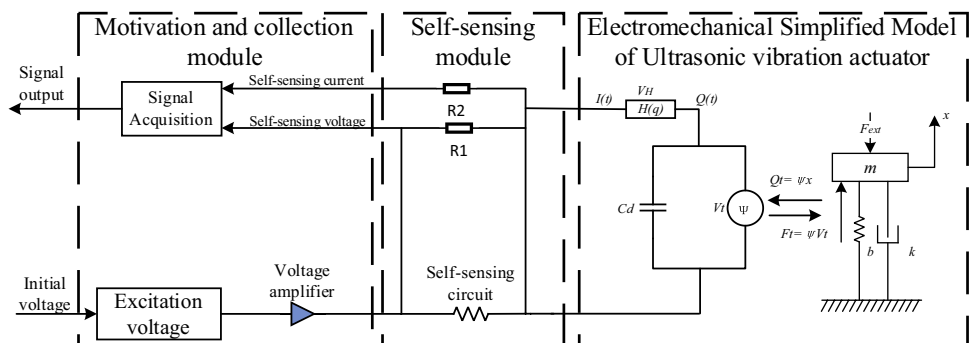
where S is mechanical strain, D is electric displacement vector, T is mechanical stress, E is electric field strength, s is flexibility constant, d is piezoelectric strain constant, and ϵ is dielectric constant. Therefore, ϵ^E and ϵ^T represent the flexible matrix and the dielectric constant, respectively. Therefore, based on this piezoelectric relationship, the self-sensing and control module for resonance was designed as shown in Fig. 17. In this method, to ensure the real-time resonance of ultrasonic vibration device during processing, in this paper, a kind of acquisition circuit for electric signals of piezoelectric ceramics is designed. It is simplified as a self-sensing module in Fig. 17.

It can be seen from Fig. 16 that the current and voltage collected by this self-sensing module is input to the control module, which monitors the vibration and controls the supply voltage of devices in real time according to the control algorithm. Since the vibration of an ultrasonic cutting device affects the machining quality of workpieces directly. To improve the vibration robustness of the device, the excitation voltage must be controlled according to closed-loop feedback. Based on the model established in the previous

Table 4 Experimental equipment for signal acquisition

Name	Type	Function
Computer	Ordinary PC	Provide an interface for parameter setting and display the result
Controller	NI-USB6361X	The operation of the control system
Signal acquisition device	Own design	Collect voltage and current signals
Voltage amplifier	TERK PZD700A	Amplify the excitation voltage signal
Micro-displacement sensor	Microsense 5504 capacitive displacement sensor	Measure the output displacement of the piezoelectric transducer
Signal conditioning module	Microsense 5300 measuring system	Process the incoming signal from the sensor

Fig. 14 Schematic diagram of self-sensing processing for ultrasonic-assisted cutting devices



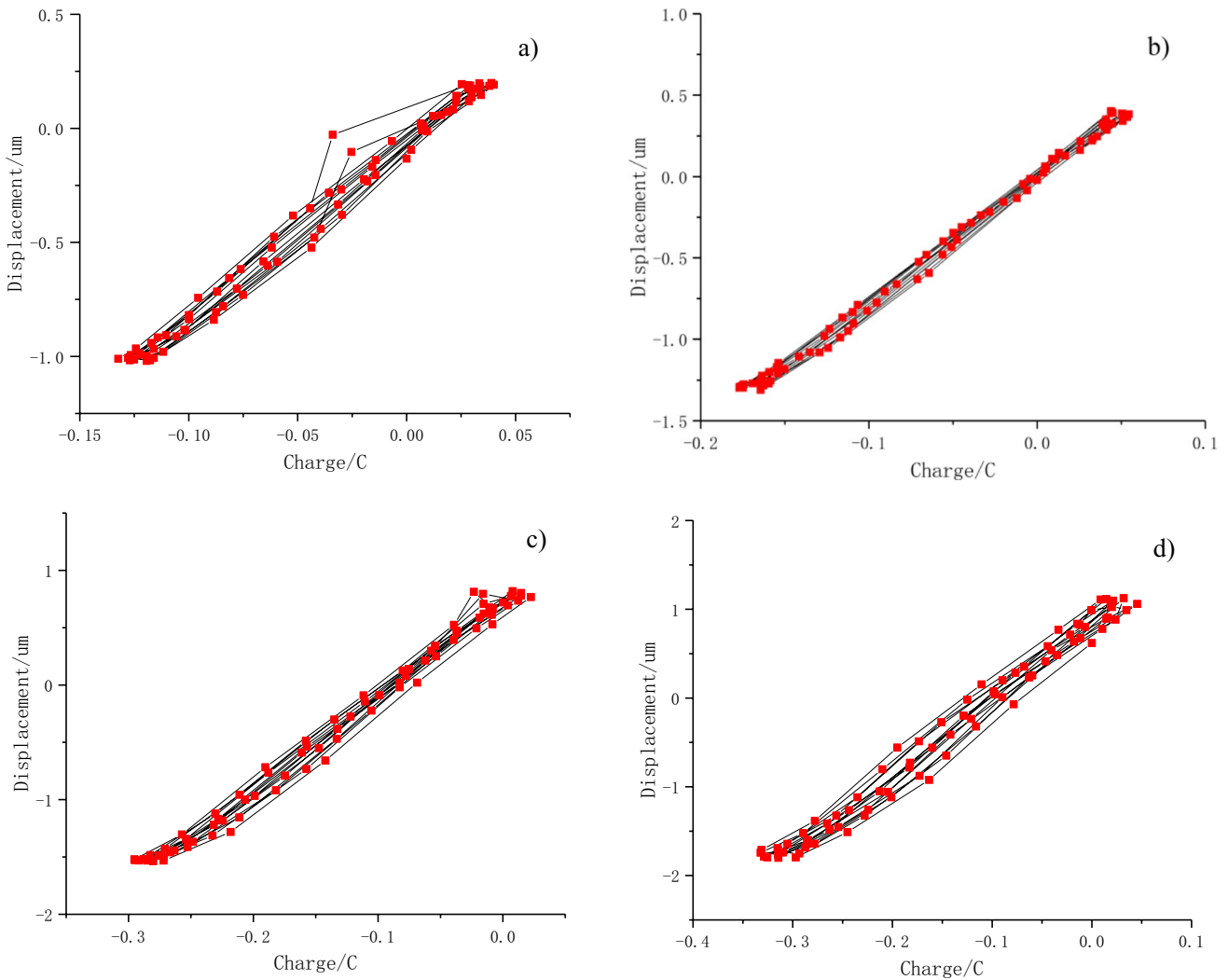


Fig. 15 Charge-displacement characteristic curves: **a** voltage amplitude 300 V, **b** voltage amplitude 400 V, **c** voltage amplitude 500 V, and **d** voltage amplitude 600 V

Table 5 Conversion factor for different voltage amplitudes

Voltage amplitude (V)	300 V	400 V	500 V	600 V
Conversion factor of two-dimensional ultrasonic elliptical vibration cutting device k ($\mu\text{m}/\text{C}$)	7.67	7.69	8.09	8.41

section, a system for self-sensing stability control of ultrasonic elliptical vibration cutting is designed. In the control module of this system, the input is the self-sensing electrical signal and the output is excitation voltage after adjustment. The schematic diagram is shown in Fig. 18.

In Fig. 18, the key of this control method lies in the acquisition and processing of voltage signal $V(t)$ and current signal $I(t)$. Using these two signals, the applied charge $Q(t)$ and the hysteresis voltage V_H can be calculated according to the electromechanical conversion model. First of all, the excitation voltage $V(t)$ and the total current $I(t)$ of this device are

extracted by the induction of resistances, which are used as the input of this controller then. Based on the hysteresis model established in Section 2, the hysteresis voltage V_H of a piezoelectric transducer can be calculated by the total current $I(t)$. Therefore, according to the corresponding conversion coefficient k , the displacement of this device is estimated, and the real-time amplitude deviation ΔA of the device is obtained. Using the amplitude deviation ΔA as input, the amplitude of devices can be tracked by the PID control algorithm.

Due to the structural characteristics of piezoelectric transducers, the maximum amplitude of a resonant device can be

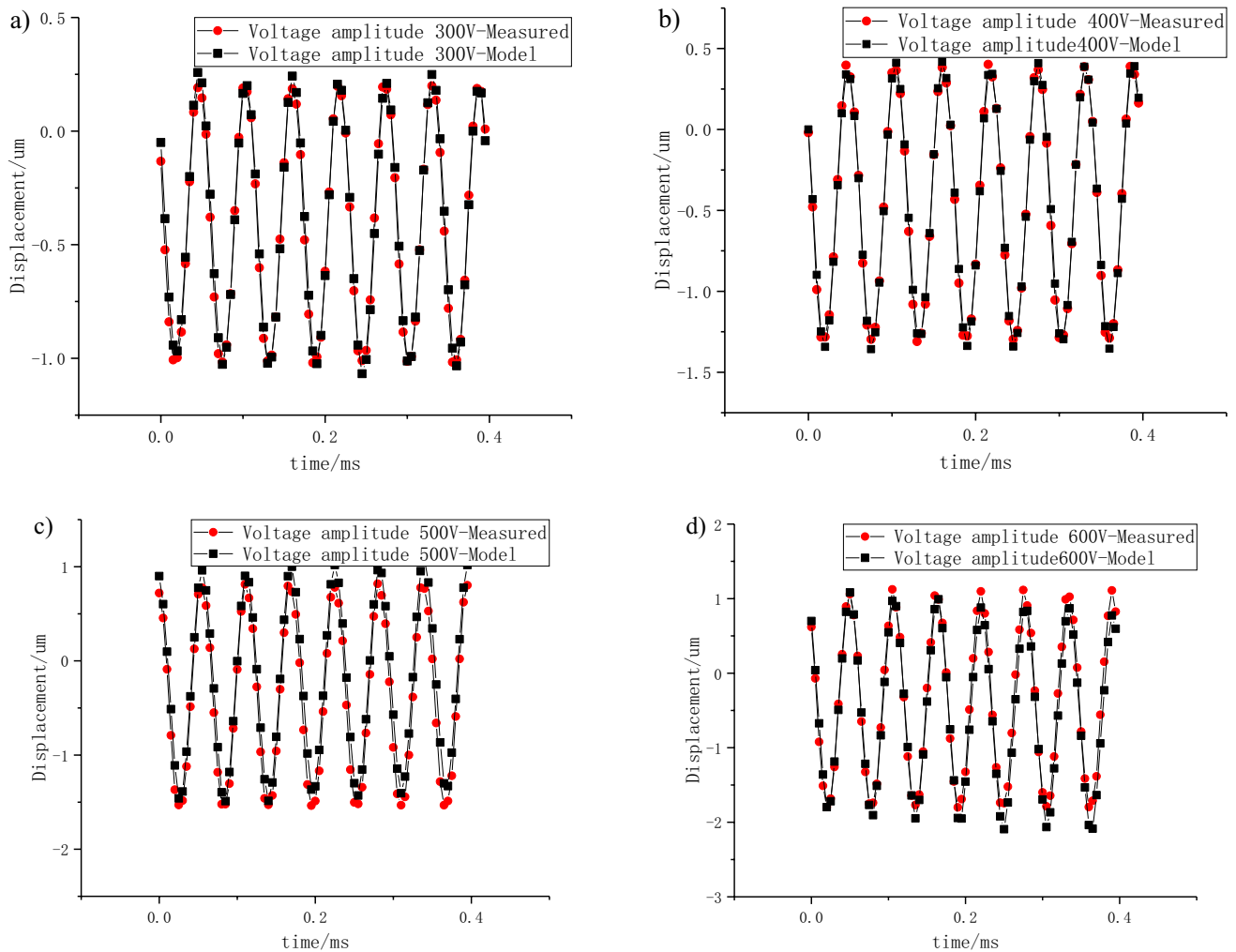


Fig. 16 Comparison of measured and estimated displacement values of different voltage amplitude: **a** voltage amplitude 300 V, **b** voltage amplitude 400 V, **c** voltage amplitude 500 V, and **d** voltage amplitude 600 V

Table 6 Comparison of actual and estimated displacements

Voltage amplitude (V)	300 V	400 V	500 V	600 V
Actual displacement amplitude (μm)	0.631	0.869	1.201	1.443
Estimated displacement amplitude (μm)	0.630	0.865	1.198	1.422
Error (%)	0.17	0.46	0.22	1.47

reached at the resonant frequency. In the actual cutting process, the vibration frequency deviates from its resonant frequency due to cutting load and other reasons. This causes the actual displacement of devices to be less than the predetermined value, which leads to the machining error. In this paper, a self-sensing monitor and control system of ultrasonic elliptical vibration cutting devices is established. According to the kinetic relationship in Fig. 1:

$$m\ddot{x} + b\dot{x} + kx = F_t + F_{ext} \tag{14}$$

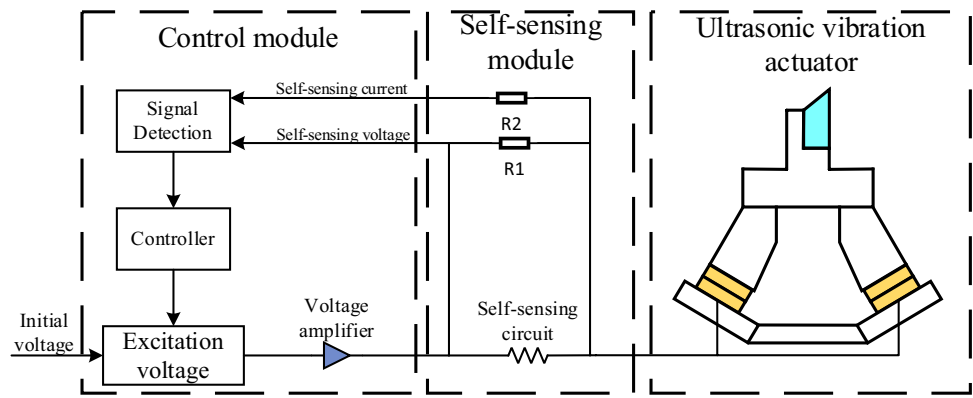
By combining Eq. (1) to Eq. (2), the transfer function between the current I_t and the supply voltage V_t is

$$G(s) = \frac{I_t(s)}{V_t(s)} = \frac{\psi^2 s}{ms^2 + bs + k}. \tag{15}$$

When the frequency of input voltage matches the natural frequency of working mode, the real part of s in this transfer function $G(s)$ is 0. Given the resonance frequency $\omega_n = \sqrt{k/m}$ and the damping coefficient $\zeta = b/(2\sqrt{mk})$, the transfer function is:

$$G_a(s) = \frac{I_t(s)}{V_t(s)} = \frac{1}{k} \frac{\psi^2 \omega_n^2 \omega}{2\zeta \omega \omega_n + j(\omega^2 - \omega_n^2)}. \tag{16}$$

Fig. 17 Schematic diagram of self-sensing-based ultrasonic vibration cutting device's frequency and amplitude stable control method



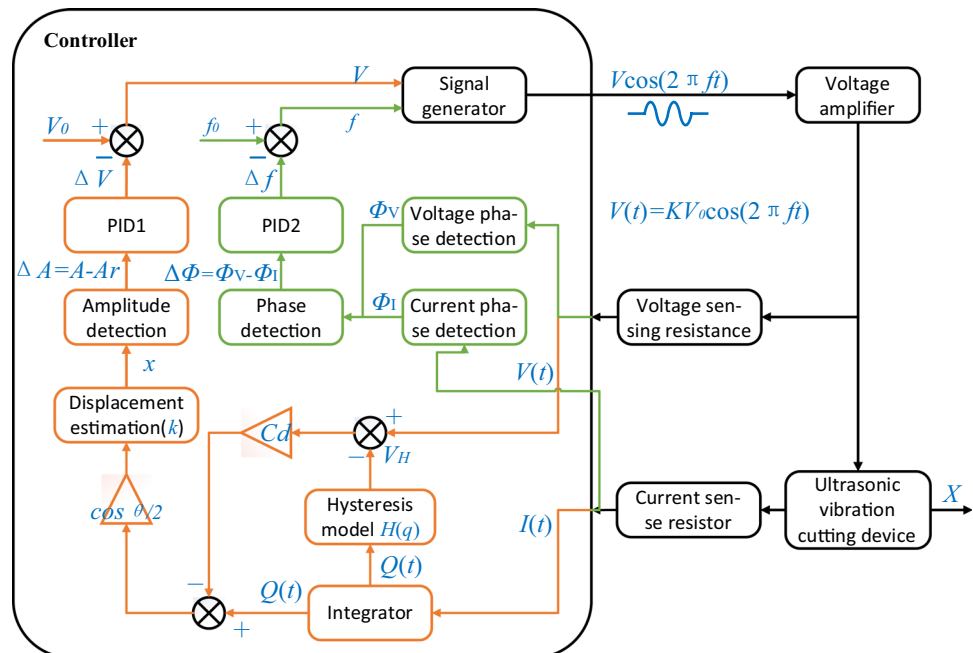
It can be seen from Eq. (16) that when the piezoelectric transducer is in resonance, that is, when $\omega = \omega_n$, the phase of the frequency response function is $\phi = \angle G_a(j\omega_n) = 0$. Therefore, by detecting the phase of the frequency response function $\phi = \angle G_a(j\omega)$, the deviation between the current vibration frequency and the resonance frequency of piezoelectric transducers is judged. The resonance control system of ultrasonic vibration cutting devices consists of two loops. One of the control loops is the amplitude control, which changes the voltage to achieve a specific displacement according to the estimated displacement. Another loop is the frequency control loop, which calculates the phase difference of self-sensing signals (such as self-sensing voltage and current) and controls the supply voltage to achieve resonance. The PID algorithm is used as an adjustment algorithm to control the frequency and amplitude of vibration. The PID controller is defined as follows:

$$\begin{cases} \Delta f(k) = \Delta f_p(k) + \Delta f_i(k) + \Delta f_d(k) \\ \Delta f_p(k) = k_{fp} e_\theta(k) \\ \Delta f_i(k) = k_{fi} \sum_{i=0}^k e_\theta(i)T \\ \Delta f_d(k) = k_{fd} \frac{e_\theta(k) - e_\theta(k-1)}{T} \end{cases} \quad (k = 1, \dots, n) \quad (17)$$

where $\Delta f(k)$ is the output of PID controller, that is, the adjusted frequency parameters, $e(k)$ is the input of PID controller, which represents deviation signal of this control system and k represents the number of sampling points, T is sampling period, and k_p , k_i , and k_d represent proportional link coefficient, integral link coefficient, and differential link coefficient of PID controller, respectively.

In the same way, the amplitude stability controller was established based on the PID control algorithm, and it is defined as follows:

Fig. 18 Schematic diagram of state stability control process in ultrasonic elliptical vibration cutting



$$\left\{ \begin{array}{l} \Delta V(k) = \Delta V_P(k) + \Delta V_I(k) + \Delta V_D(k) \\ \Delta V_P(k) = k_{Vp} e_A(k) \\ \Delta V_I(k) = k_{Vi} \sum_{i=0}^k e_A(i) T \\ \Delta V_D(k) = k_{Vd} \frac{e_A(k) - e_A(k-1)}{T} \end{array} \right. \quad (k = 1, \dots, n). \quad (18)$$

Generally, the parameters of these PID controllers need to be identified in parameter identification experiments. In this paper, a series of PID controller parameter identification experiments were performed to obtain the necessary control parameters.

5 Validation experiments

In this paper, a comparison experiment with and without the self-sensing control system was carried out to verify the accuracy of this system. This experiment was tested in JDGR 400 T A13S machining center. The machining object is cylindrical rods of aluminum alloy. The tool parameters are shown in Table 7.

The cutting experiment of micro-pit structure is a kind of machining process that can fully reflect vibration error. It is used as a method to evaluate the quality of the ultrasonic vibration process. Before cutting the micro-pit structure, a pre-machining was performed to obtain a smooth cylindrical surface (the machine speed was 5000 r/min, the feed speed was 20 mm/min). Subsequently, the experiment of ultrasonic elliptical-vibration cutting of micro-pits on the cylindrical surface was performed. The processing parameters are shown in Table 8.

After processing, the micro-structure of these workpiece surfaces was measured with the HIROX KH-7700 three-dimensional digital microscope. The measurement results are shown in Fig. 19.

It is not difficult to see from Fig. 18 that the surface quality of ultrasonic vibration processing with self-sensing monitoring and control system is much better than that without the system. The geometry of machined micro-pit structures with this system is closer to the theoretical value and smoother. While the cutting processing of micro-pits is a compound movement, the arrangement of micro-pits on the surface was offset in the axial direction. To evaluate the machining quality with or without the system quantitatively, the errors of morphology and position were measured as shown in Table 9.

In Table 9, we set the distance between the lowest point of two micro-pits to represent its position, and the distance between the highest point of two micro-pits represents its morphology. Table 9 shows the comparison between the measurement data and theoretical values of micro-pit in the experiments of 1–5 and 1–6. It can be easily seen from the table that without this self-sensing monitoring and control

system, the error of shape size and distribution size are relatively large; in particular, the error of the circumferential length reaches 23.48%. By using the self-resonant control proposed in this paper, the circumferential length error of morphology is reduced by 11.47%. The other errors show varying degrees of reduction except for the axial error of position. Although the error of the axial distance is relatively small, it could not be used as an evaluation index of control results. Because the axial distance is only related to the feed speed of the machine tool and the spindle speed. However, in the case that the micro-pits were processed by using the self-sensing monitoring and control system proposed in this paper, the error of shape size and distribution size are significantly reduced. The improvement in circumferential length and depth is the most obvious, and the amplitude and frequency of vibration are stabilized at the predetermined value. Therefore, the self-sensing monitoring and control system for ultrasonic cutting devices considering the hysteresis effect proposed in this paper is effective.

6 Conclusion

The resonance robustness in ultrasonic vibration cutting is the focus of this paper. Due to the contact between the tool and the workpiece during machining, the actual resonance frequency does not match the frequency of the excitation voltage. To solve this problem, a self-sensing monitoring and control system considering the hysteresis effect is designed. After model comparison and actual processing experiments, the conclusion is as follows:

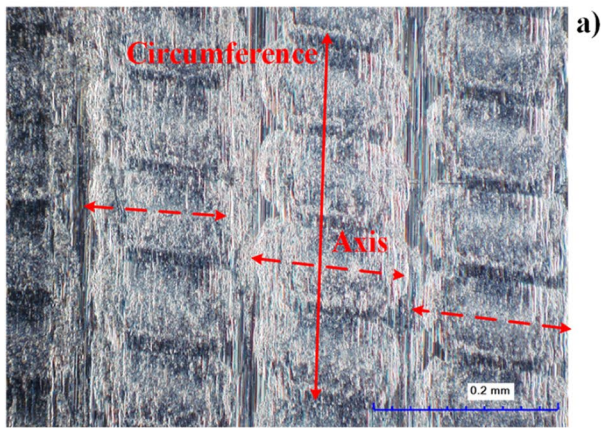
1. To monitor the vibration of ultrasonic vibration devices in real time, a self-sensing monitoring system was developed to monitor real-time electrical signals of piezoelectric ceramics in the cutting process. A monitor experiment of piezoelectric ceramics showed that the self-sensing voltage and measured displacement conformed to the laws of piezoelectric characteristics in piezoelectric ceramics. It proved that the signal collected and processed by the self-sensing monitoring system can reflect the real-time vibration of piezoelectric ceramics.
2. Aiming to solve the problem that the hysteresis error of the ultrasonic elliptical vibration cutting device is difficult to compensate, the PI model was used to model the hysteresis effect. By comparing simulated data and

Table 7 Parameters of carbide turning tools

Name	Tool material	Type	Rake angle	Clearance angle
Turning tool	Cemented carbide	DCGT070204R-F	0°	7°

Table 8 Machining parameters of cylindrical micro-pits in ultrasonic elliptical vibration cutting

Number	With or without control	Depth of cut (μm)	Excitation voltage (V)	Spindle speed (r/min)	Feed speed (mm/min)
1–5	Without	5	400	3500	630
1–6	With				



measured data of charge-hysteresis voltage, the experimental results show that the PI model could properly describe the piezoelectric hysteresis effect of ultrasonic vibration devices. When the voltage is 400 V, the error of the PI model reached the peak value, and the maximum relative error was 16%.

- Based on the piezoelectric effect of piezoelectric ceramics, the electro-mechanical conversion model of ultrasonic elliptical vibration devices was established. The comparison between model simulation and experimental

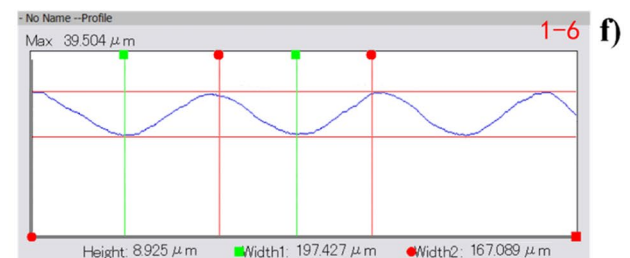
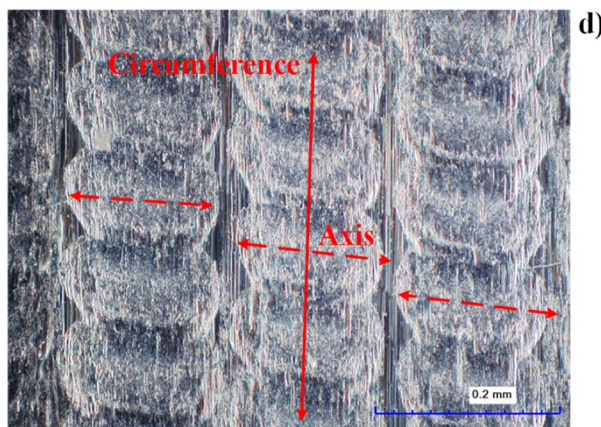
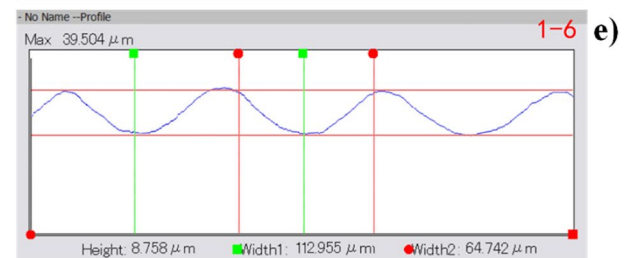
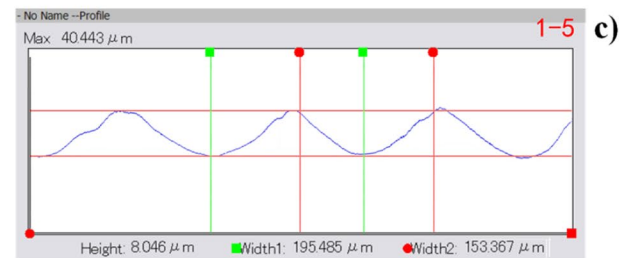
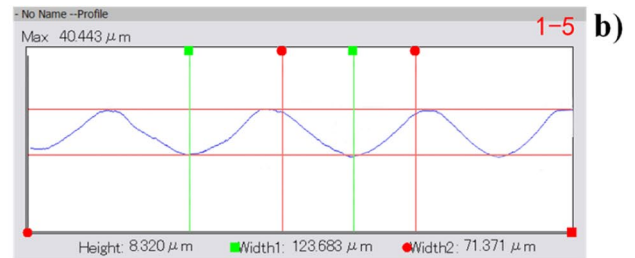


Fig. 19 Comparison of micro-texture topography with or without self-sensing control: **a** without self-sensing control, **b** circumferential topography without self-sensing, **c** axial topography without self-

sensing, **d** with self-sensing control, **e** circumferential topography with self-sensing, and **f** axial topography with self-sensing

Table 9 The comparison between the corresponding micro-pit measurement data and calculated theoretical values

Parameter	Morphology			Position	
	Depth	Circumference	Axis	Circumference	Axis
Theoretical values in experiment 1–5 and 1–6	9 μm	57.8 μm	177.76 μm	99.6 μm	180 μm
Measured values in experiment 1–5	8.32 μm	71.37 μm	153.37 μm	123.68 μm	195.49 μm
Relative error in experiment 1–5	7.56%	23.48%	13.72%	24.18%	8.61%
Measured values in experiment 1–6	8.76 μm	64.74 μm	167.09 μm	112.96 μm	197.43 μm
Relative error in experiment 1–6	2.67%	12.01%	6.00%	13.41%	9.68%
Error comparison between experiment 1–5 and 1–6	–4.89%	–11.47%	–7.72%	–10.77%	1.07%

measurement showed that within the range of voltage amplitude measured in this paper, the electro-mechanical model established showed a maximum error of 1.47%, showing quite high accuracy.

- According to the actual displacement estimation model of this ultrasonic vibration cutting system established in this paper, a real-time self-sensing monitoring and control system of ultrasonic vibration cutting devices was developed. Through the micro-structure cutting experiment, it was found that when the micro-pits were processed by using the self-sensing monitoring and control system established in this paper, the robustness of vibration is significantly improved and the errors of vibration with cutting load were significantly reduced.

Acknowledgements The authors are thankful to reviewers for their comments and suggestions to improve the quality of the manuscript.

Author contribution Fuhang Yu: hysteresis compensation, experiments, data collection, and manuscript writing. Chen Zhang: methodology, concept, and thought guide. Xiaoming Gan: control method and experiments. Xin Hu: experiments and data processing. All authors read and reviewed the manuscript.

Funding The work in this paper was supported by the National Natural Science Foundation of China (NSFC) under Grant Number 51675277 and by the High-Level Talents Project of “Six Talents Summit” in Jiangsu under Grant Number GDZB-011.

Declarations

Conflict of interest The authors declare no competing interests.

References

- Feng Y, Hsu F, Lu Y, Lin Y, Lin C, Lin C, Lu Y et al (2021) Force prediction in ultrasonic vibration-assisted milling. *Mach Sci Technol* 25:307–330. <https://doi.org/10.1080/10910344.2020.1815048>
- Feng Y, Hsu F, Lu Y, Lin Y, Lin C, Lin C, Lu Y et al (2020) Temperature prediction of ultrasonic vibration-assisted milling. *Ultrasonics* 108:106212. <https://doi.org/10.1016/j.ultras.2020.106212>
- Zhang J, Cui T, Ge C, Sui Y, Yang H (2016) Review of micro/nano machining by utilizing elliptical vibration cutting. *Int J Mach Tools Manuf* 106:109–126. <https://doi.org/10.1016/j.ijmactools.2016.04.008>
- Feng Y, Hsu F, Lu Y, Lin Y, Lin C, Lin C, Lu Y et al (2020) Tool wear rate prediction in ultrasonic vibration-assisted milling. *Mach Sci Technol* 24:758–780. <https://doi.org/10.1080/10910344.2020.1752240>
- Devasia S, Eleftheriou E, Moheimani SR (2007) A survey of control issues in nanopositioning. *IEEE Trans Control Syst Technol* 15:802–823. <https://doi.org/10.1109/TCST.2007.903345>
- Hubbard NB, Culpepper ML, Howell LL. (2006) Actuators for micropositioners and nanopositioners. *Applied Mechanics Reviews*, 59. <https://doi.org/10.1115/1.2345371>
- Chua ZY, Ahn IH, Moon SK (2017) Process monitoring and inspection systems in metal additive manufacturing: Status and applications. *Int J Precis Eng Manuf Green Technol* 4:235–245. <https://doi.org/10.1007/s40684-017-0029-7>
- Woronko A, Huang J, Altintas Y (2003) Piezoelectric tool actuator for precision machining on conventional CNC turning centers. *Precis Eng* 27:335–345. [https://doi.org/10.1016/S0141-6359\(03\)00040-0](https://doi.org/10.1016/S0141-6359(03)00040-0)
- Shamoto E, Suzuki N, Moriwaki T, Naoi Y (2002) Development of ultrasonic elliptical vibration controller for elliptical vibration cutting. *CIRP Ann* 51:327–330. [https://doi.org/10.1016/S0007-8506\(07\)61528-5](https://doi.org/10.1016/S0007-8506(07)61528-5)
- Yin Z, Fu Y, Xu J, Li H, Chen Y (2017) A novel single driven ultrasonic elliptical vibration cutting device. *Int J Adv Manuf Technol* 90:1–12
- Bazghaleh M, Grainger S, Mohammadzahari M, Cazzolato B, Lu T (2013) A digital charge amplifier for hysteresis elimination in piezoelectric actuators. *Smart Mater Struct* 22:75016. <https://doi.org/10.1088/0964-1726/22/7/075016>
- Newcomb CV, Flinn I (1982) Improving the linearity of piezoelectric ceramic actuators. *Electron Lett* 18:442–444. <https://doi.org/10.1049/el:19820301>
- Minase J, Lu T, Cazzolato B, Grainger S (2010) A review, supported by experimental results, of voltage, charge and capacitor insertion method for driving piezoelectric actuators. *Precision Engineering* 34:692–700. <https://doi.org/10.1016/j.precisioneng.2010.03.006>
- Ryba Ł, Dokoupil J, Voda A, Besançon G (2017) Adaptive hysteresis compensation on an experimental nanopositioning platform. *Int J Control* 90:765–778. <https://doi.org/10.1080/00207179.2016.1214874>
- Tanaka Y, Kokubun Y, Yabuno H (2018) Proposition for sensorless self-excitation by a piezoelectric device. *J Sound Vib* 419:544–557. <https://doi.org/10.1016/j.jsv.2017.11.033>
- Chen L, Yen J, Chen JJ, Kuo F, Chen M, Chen Y, Chung B (2013) Precision tracking of a piezo-driven stage by charge feedback control. *Precis Eng* 37:793–804. <https://doi.org/10.1016/j.precisioneng.2013.03.002>

17. Liaw HC, Shirinzadeh B, Smith J (2007) Enhanced sliding mode motion tracking control of piezoelectric actuators. *Sens Actuators, A* 138:194–202. <https://doi.org/10.1016/j.sna.2007.04.062>
18. Zhu Z, To S, Li Y, Zhu W, Bian L (2018) External force estimation of a piezo-actuated compliant mechanism based on a fractional order hysteresis model. *Mech Syst Signal Process* 110:296–306. <https://doi.org/10.1016/j.ymssp.2018.03.012>
19. Zhang X, Lu Z, Peng Z, Sui H, Zhang D (2018) Development of a tool-workpiece thermocouple system for comparative study of the cutting temperature when high-speed ultrasonic vibration cutting Ti-6Al-4V alloys with and without cutting fluids. *Int J Adv Manuf Technol* 96:237–246. <https://doi.org/10.1007/s00170-018-1600-2>
20. Gao J, Caliskan H, Altintas Y (2019) Sensorless control of a three-degree-of-freedom ultrasonic vibration tool holder. *Precis Eng* 58:47–56. <https://doi.org/10.1016/j.precisioneng.2019.05.005>
21. Mansour SZ, Seethaler RJ (2017) Simultaneous displacement and force estimation of piezoelectric stack actuators using charge and voltage measurements. *IEEE/ASME Trans Mechatron* 22:2619–2624. <https://doi.org/10.1109/TMECH.2017.2757931>
22. Zhang H, Gao R, Zhang H, Wu C (2022) Effect of mechanical compliance of mounting clamp on electrical properties and vibration response of high-frequency piezoelectric ultrasonic transducer for microelectronic packaging and interconnection. *Sensors Actuators A: Phys* 335:113374. <https://doi.org/10.1016/j.sna.2022.113374>
23. Yang J, Feng P, Zhang J, Wang J (2022) Design optimization of ultrasonic vibration cutting tool to generate well-decoupled elliptical trajectory. *Int J Adv Manuf Technol* 119:7199–7214
24. Ge P, Jouaneh M (1996) Tracking control of a piezoceramic actuator. *IEEE Trans Control Syst Technol* 4:209–216. <https://doi.org/10.1109/87.491195>
25. Viswamurthy SR, Ganguli R (2007) Modeling and compensation of piezoceramic actuator hysteresis for helicopter vibration control. *Sens Actuators, A* 135:801–810. <https://doi.org/10.1016/j.sna.2006.09.020>
26. Al Janaideh M, Rakheja S, Su C (2010) An analytical generalized Prandtl-Ishlinskii model inversion for hysteresis compensation in micropositioning control. *IEEE/ASME Trans Mechatron* 16:734–744. <https://doi.org/10.1109/TMECH.2010.2052366>
27. Rakotondrabe M (2010) Bouc-Wen modeling and inverse multiplicative structure to compensate hysteresis nonlinearity in piezoelectric actuators. *IEEE Trans Autom Sci Eng* 8:428–431. <https://doi.org/10.1109/TASE.2010.2081979>
28. Lin C, Lin P (2012) Tracking control of a biaxial piezo-actuated positioning stage using generalized Duhem model. *Comput Math Appl* 64:766–787. <https://doi.org/10.1016/j.camwa.2011.12.015>
29. Xu Q (2012) Identification and compensation of piezoelectric hysteresis without modeling hysteresis inverse. *IEEE Trans Industr Electron* 60:3927–3937. <https://doi.org/10.1109/TIE.2012.2206339>

Publisher's Note Springer Nature remains neutral with regard to jurisdictional claims in published maps and institutional affiliations.

Springer Nature or its licensor (e.g. a society or other partner) holds exclusive rights to this article under a publishing agreement with the author(s) or other rightsholder(s); author self-archiving of the accepted manuscript version of this article is solely governed by the terms of such publishing agreement and applicable law.